RELIABILITY AND PROGRESSIVE DAMAGE MODELING OF COMPOSITE STRUCTURES WITH MANUFACTURING DEFECTS

Jared W. Nelson, Trey W. Riddle, W. Matt Peterson, and Douglas S. Cairns
Montana State University
Bozeman, MT, 59717

ABSTRACT

Manufacturing of composite structures is often developed to meet design constraints based on system optimization that may result in uncertain reliability through the design life due to the inclusion of manufacturing related defects. Assumptions are often made for worst case scenarios with modeling techniques instead of modeling actual defect geometry. To address these issues, a framework for composite structure reliability with an emphasis on progressive damage modeling and probabilistic analysis has been developed. Probabilistic analysis assesses the probability of failure while taking into account load conditions and structural defect data allowing for Criticality Assessment development to evaluate the in-use risks of a structure with manufacturing defects. While in operation, Reliability Estimation is continually performed to assess, validate, and continually update the Criticality Assessment. To support this framework both a combined continuum/discrete and a novel multipoint constraint cohesive zone approaches were developed to analyze typical manufacturing defects. Overall, validation was achieved by testing a subscale wind turbine blade containing representative manufacturing defects with results proving that this methodology provides quantification of the effects of manufacturing defects for improved reliability of composite structures.

1. INTRODUCTION & BACKGROUND

Given the size and weight of wind turbine blades, advanced composite materials have become an optimal choice due to their high strength-to-weight ratio. These materials are also attractive because of the ability to form the complex shapes required for rotor aerodynamics combined with relatively low-cost manufacturing [1]. However, many of the blade suppliers are using technologies and techniques derived from those developed for structures with much lower design loads and criteria. While these methods have been continuously improving, blades are large complex parts that have been designed for cost and functional efficiency and not necessarily for manufacturability. Thus, it is not clear that such improvements have been developed at a rate necessary to ensure reliability over a desired 20 year design life [2].

The Department of Energy sponsored Blade Reliability Collaborative (BRC) has been formed to better understand what is needed to improve wind turbine blade reliability through a comprehensive study characterizing and understanding typical blade-related manufacturing flaws.[3] Led by Sandia National Laboratories, the BRC is made up of a collaborative of wind farm owners/operators, turbine manufacturers and third party investigators. The BRC has charged the Montana State University Composites Group (MSUCG) with the goal "to understand and quantify the effects of manufacturing discontinuities and defects with respect to wind turbine blade structural performance and reliability." Two coordinated distinct tasks, Flaw

Characterization and Effects of Defects, were established to meet this goal and the work is summarized herein. The former, Flaw Characterization, has focused on performing mechanical testing of flawed composite specimen and developing probabilistic models to assess the reliability of a wind blade with defects. The latter has focused on developing predictive progressive damage models for correlation with experimental test results. More generally, this allows for a unique comparison of different analytical approaches to model progressive damage in composite laminates with typical manufacturing defects for consistency, accuracy, and predictive capability to allow for improved composite structural assessment. In conjunction, a novel method to assess 3D structures utilizing cohesive element has been investigated.

1.1 Benchmark Experimental Overview

Three composite laminate defect types were deemed critical by BRC members to blade function and life cycle: in-plane (IP) waves, out-of-plane (OP) waves, and porosity/voids. While extensive studies have reported on each of the defect types in thin laminates utilizing varying advanced composite materials, less research has been performed for wind turbine blade materials and representative defects [1]. Further, it must be noted that much of this research has been performed for industries where manufacturing is on a smaller scale, where expense is less critical. Most of this prior research offers a preliminary basis for this work, but it is known that acceptable defects often included in wind turbine blades far exceed what would be acceptable in other industries, such as aerospace. Thus, research specific to understanding the criticality of defects common to blades is necessary. A repeatable metric for defect data acquisition, image processing, defect characterization, and statistical analysis has been developed to precisely address the geometric nature of flaws based on statistical commonality in blades. In order to do this several commercial scale wind turbine blades were reviewed. Examples of these flaw types from utility scale wind turbine blades are shown in Figure 1-3 [3].

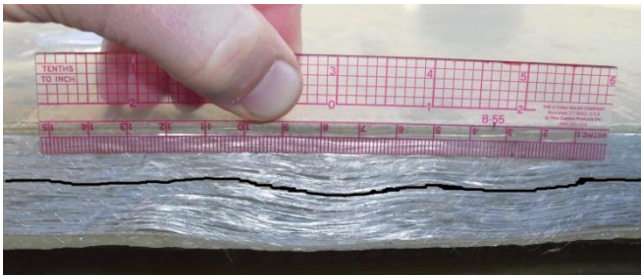

Figure 1. Image of Out of Plane wave

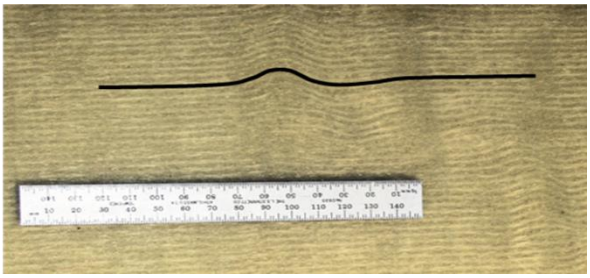

Figure 2. Image of In-Plane wave

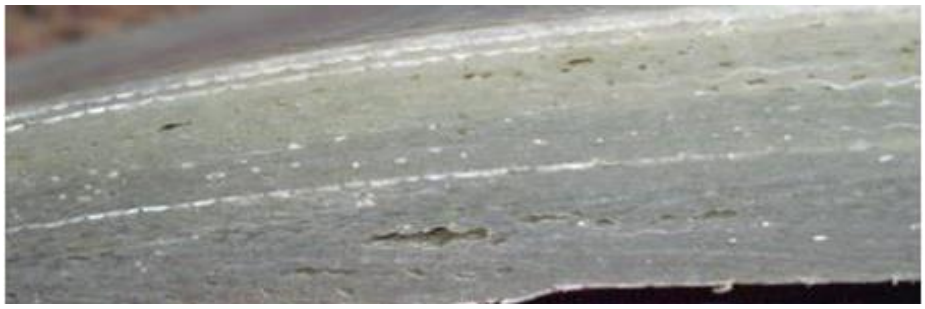

Figure 3. Image of porosity and voids

Results from the flawed blade field survey, completed testing program on flawed laminate coupons, the extensive MSUCG composites database and published data from other investigators work have provided data for probabilistic analysis input distributions. [4] An example of the flaw magnitude distribution for IP waves is given in Figure 4. Here it can be seen that off-axis fiber misalignment angle of surveyed flaws trends well with typical statistical distributions. Similar data was collected on OP waves.

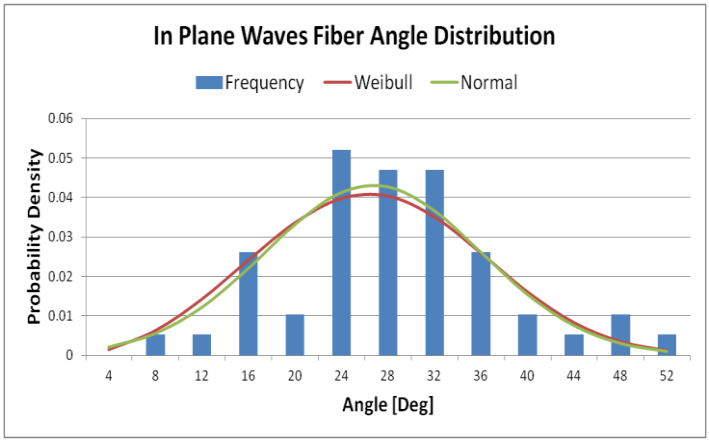

Figure 4: In plane wave fiber angle distribution.

Representative flaws were tested on a coupon scale in quasi-static tension and compression. An example of the reduced ultimate strength of a laminate with flaws is given in Figure 5, left. In all cases, failure strengths and strains were correlated to the characteristic flaw parameter. An example of the knockdown factor data and trend for IP waves is shown in Figure 5, right. Complete detail may be found in previous work performed by the authors [4].

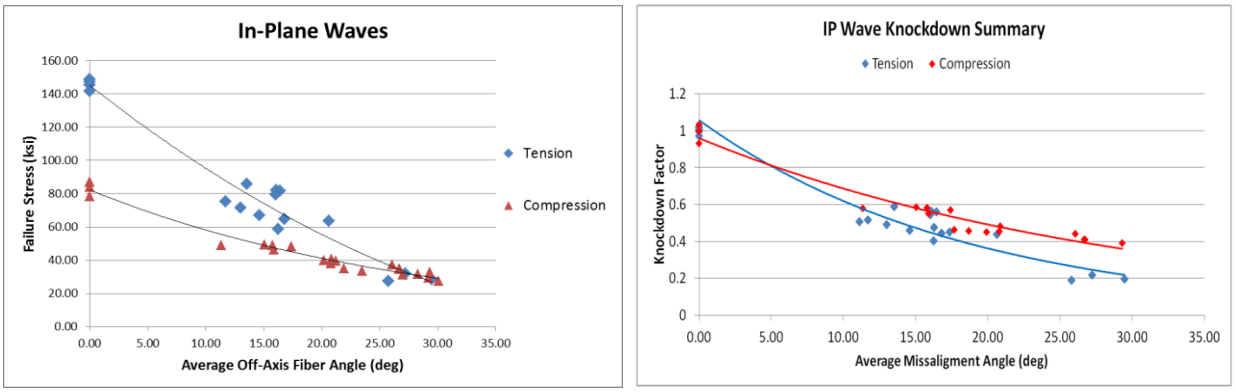

Figure 5. Failure strain for In-Plane waves (left) and knockdown factors for IP Waves (right).

2. MANUFACTURING DEFECTS AS UNCERTAINTY VARIABLES

2.1 Model Overview

Variations in the structural behavior of composites cannot be characterized by traditional deterministic methods utilizing safety factors to account for uncertain structural response. Moreover, lightweight composite materials are known to be sensitive to fatigue and defects or damage. Therefore, a methodology focused on reliability targets, which incorporates probabilistic modeling, is essential to accurately determine the structural reliability of a composite structure. A block diagram describing the interaction of the various components of this analysis are shown in Figure 6. Details for these components may be found in previous publications [4].

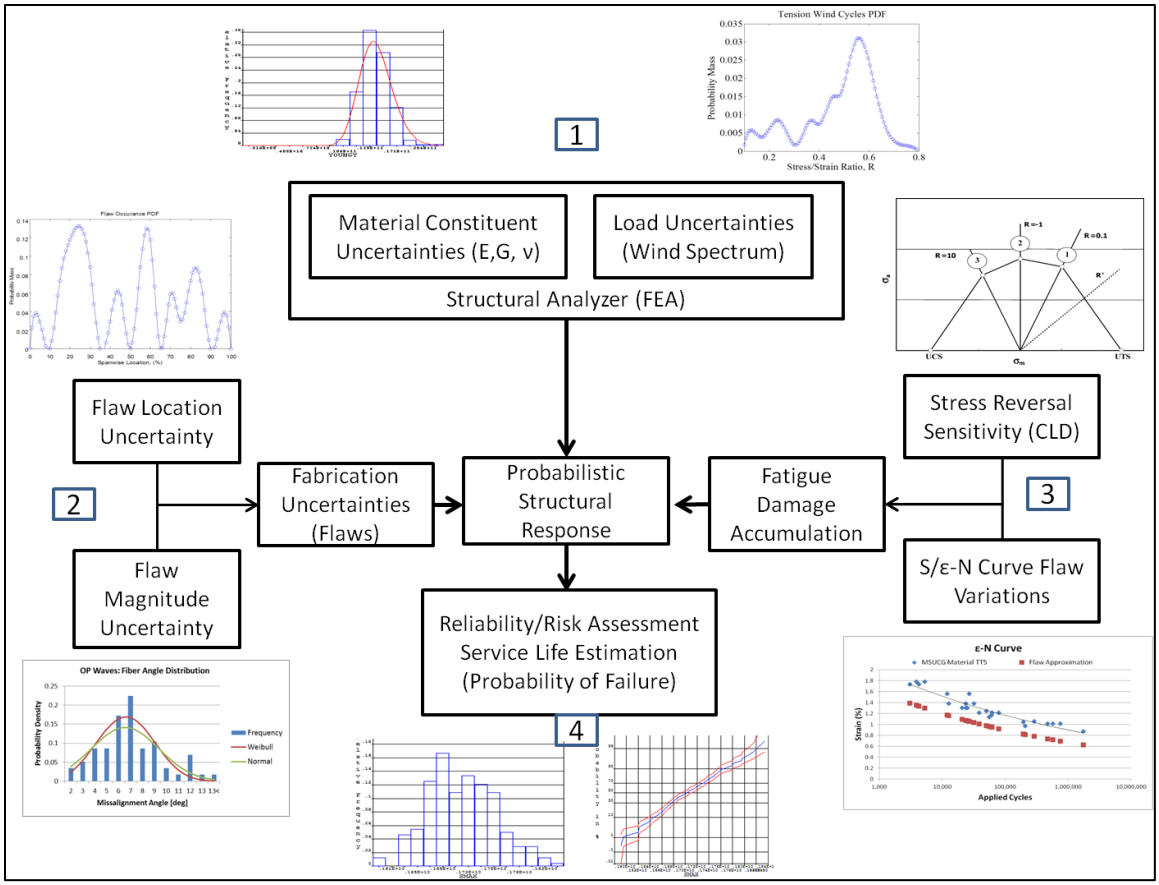

Figure 6. Analysis Information Flow

2.2 Definition of a Performance Function

Composite structures are sensitive to fatigue and spectrum loading. Application of these loading scenarios to design and testing is unreasonable; therefore, rain-flow counting is typically used to convert a spectrum loads into a set of cycles. The fatigue life can then be used in conjunction with the Palmgren-Miner's rule for linear damage accumulation [5]. A commonly used model for the fatigue life of composites is the power law [6]. The modified equation for flaw fatigue life is given in Equation 1:

$$\boldsymbol{S = KAN^{b}} \qquad [1]$$

where *S* is the maximum applied stress (or strain) N is the number of fatigue cycles, *A* is the power lower fit coefficient (often referred to as the single cycle intercept), *b* is the fit parameter for the power law slope, and *K* is the flaw knockdown factor. The natural extension to this discussion is then to translate a design life of years into cycles. The compact limit state function shown in Equation 2 can then be constructed:

$$\boldsymbol{g(X) = 1 - D(X) = 1 - \sum_{i=1}^{k} \frac{\Delta n(\varepsilon_i)}{N(\varepsilon_i)}} \qquad [2]$$

wherein the resulting strain (ε_i) is a function of the uncertainty parameter vector $\boldsymbol{X}$. The power of this formulation is it its ability model any fatigue loading spectrum and in its flexibility to predict failure as a function of applied cycles. Based on this estimation, the performance function can be evaluated two ways: assessing the probability of failure for a specific design life (e.g. 20 years) or assessing the time to failure based on an acceptable probability of failure value.

2.3 Case 1: Probability of Occurrence

Case 1 utilizes two probability distributions to describe defect uncertainty. The first distribution used in the analysis is Probability of Occurrence. This distribution describes the probability mass of a flaw existing in a blade through the use of a spatial distribution. For this analysis a 1-D distribution was used to allow for flaws down the length of the spar cap. If a flaw exists, then a second distribution is used to describe the magnitude of the flaw based on the collected in-service flaw data described above.

2.4 Case 2: Half Gaussian Magnitude

This analysis case utilizes only one probability distribution to describe defect uncertainty. The analysis assumes that there is a 100% chance of a flaw occurring at every location in the blade. Flaw occurrence magnitude is described by a one sided probability distribution. A flaw magnitude of zero (highest frequency) would indicate that there is actually no flaw. For this case, the variable to be considered for the probabilistic analysis is the flaw magnitude.

2.5 Case 1: Spatially Varying PFO

As shown in Figure 7, the Probability of Failure (P_f) by location down the length of the blade when applying the standard IEC safety factors (1.3) to the FEA simulation output strains and treating defects as random variables. Considering the time dependant formulation of linear fatigue damage accumulation (based on number of cycles), P_f may also be described as a function of time in service. It may be inferred by these results that there is a significant chance of failure, demonstrating that when using the SF with a probabilistic simulation of defects the blade will end up being overdesigned to achieve an acceptable probability of failure.

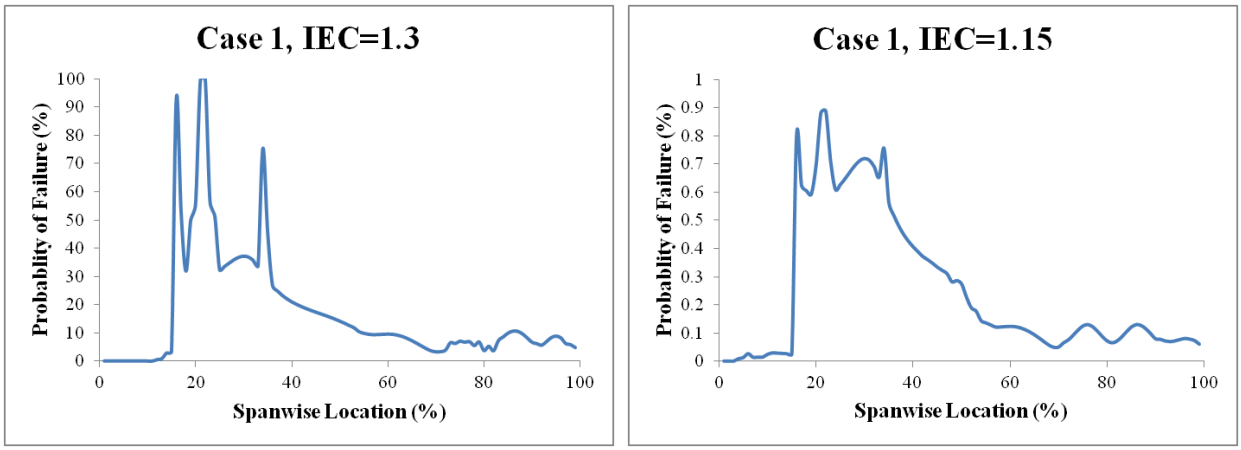

Figure 7. P_f by location (left) and P_f as a function of time for location 22 (right).

The analysis can then be repeated by reducing the IEC Material Safety Factor (γ_m) to 1.15. The results from this analysis are displayed in Figure 7, right. With the reduced SF, the P_f is significantly lowered, thereby eliminating the need for additional structural reinforcements due to additional uncertainty. This has significant implications for reducing weight and cost while providing quantifiable reliability estimation for wind turbine blades.

2.6 Case 2: Half Gaussian Magnitude Results

The same analysis can be performed using the Half Gaussian approach. The results of the probabilistic analysis both with the standard IEC SF (left) and with the reduced SF (right) are displayed in Figure 8. Once again the conservatism of the IEC SF approach can be interpreted in the same manner as Case 1 with similar weight and cost reduction implications.

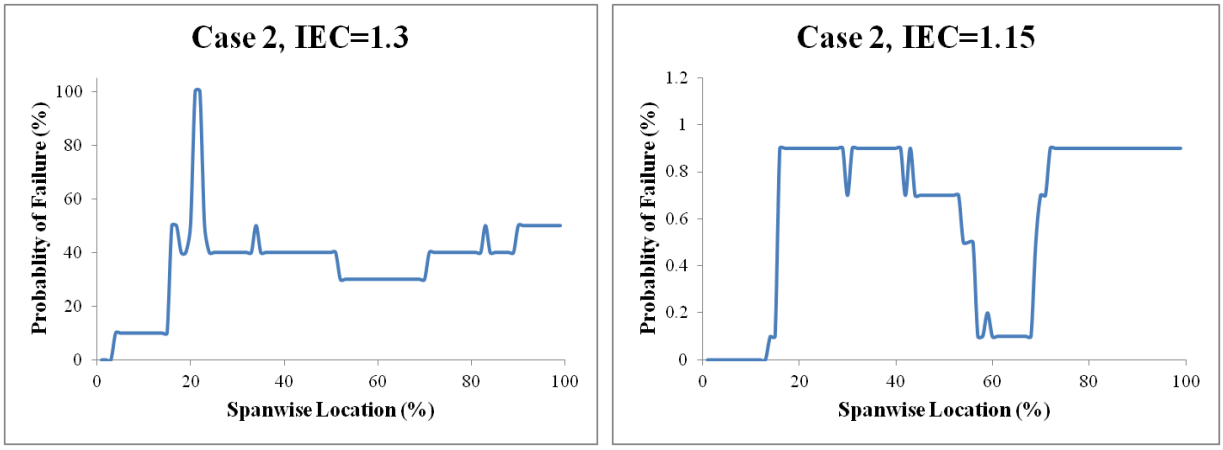

Figure 8. P_f by location with IEC SF (left) and P_f with the reduced SF (right).

2.7 Discussion

It is difficult to make a one-to-one comparison between conventional analyses or certifications of structures and the probabilistic approach presented herein. However, important comparisons were made to illustrate several points for the advantage of these analyses. If there are manufacturing defects outside of the database used for certification, it can be shown that premature failure may occur, resulting in a lifetime much shorter than the design even with an applied safety factor. This implies that the safety factor approach is not necessarily conservative and may not accomplish its intent. It has been shown that, if a probabilistic approach is taken, safety factors may be decreased resulting in more efficient wind turbine blade structures. This has the additional advantage in that the reliability can be quantified as opposed to simply assuming the safety factor will accommodate all unknowns.

For this analysis, it was not known what acceptable probability of failure was implied in the IEC safety factors. However, it can be assumed that there was an intended low probability of failure over the 20 year lifetime. A scheme was used that compares a baseline analysis that has an assumed low probability of failure. The probability that failure is reached within the 20 year lifetime with manufacturing flaws which are not inherent in the certification process. While the results are presented as probabilities of failure, they are in fact the probability of reaching the implied probability of failure as designated by the safety factor approach. In a sense, this is a relative probability of failure which allows for the comparison to the two techniques. If the

original design probability of failure is known, the absolute probability of failure could be tracked as easily through the 20 year life. Both Case 1 and 2 were evaluated with the use of the prescribed IEC safety factors and with a reduced material safety factor. This treatment allows for comparison of the conservatism in the safety factor approach. These results provide impetus for manufacturers to track and quantify manufacturing defects and probabilities. With this information, more efficient designs with quantifiable reliability are possible [4].

3. PROGRESSIVE DAMAGE MODELING

Progressive damage models were developed to assess the effects of defects of manufacturing defects in conjunction with the development of uncertainty variables. Two distinct modeling methods have been investigated and compared through the entire BRC project: Continuum Damage Modeling (CDM), and Discrete Damage Modeling (DDM). CDM is a "pseudo-representation" that does not model the exact damage, but instead updates the constitutive properties as damage occurs. As the model iterates at each strain level, the constitutive matrix is updated to reflect equilibrium damage. In contrast, a DDM physically models the damage as it occurs through the load profile, and is generally computationally more expensive. In addition, more time must also be spent in mesh creation and prior knowledge of crack path is often helpful. However, both options have shown promise for modeling composite materials [7,8].

3.1 Systematic Approach

A systematic approach was employed to compare different modeling methods discussed herein (Figure 9) for each of the models utilized. For each different model method, flaw complexity was increased, starting with a consistent unflawed case and initial IP wave case, until the correlation was deemed acceptable or unacceptable. Acceptable modeling methods were able to predict and match flawed material response for multiple flaw types utilizing unflawed material properties and flaw geometries. It is worth noting that a qualitative/quantitative approach was utilized herein that is similar to that utilized by Lemanski et al., though strains at peak stress were also considered [9]. In short, acceptable models correlated well both qualitatively, by matching failure location and shape, and quantitatively, by matching initial stiffness and peak stress at failure strain. As shown in Figure 9, if correlation was not achieved by a model at any point during the systematic increase in flaw complexity, the model was deemed unacceptable and was discarded.

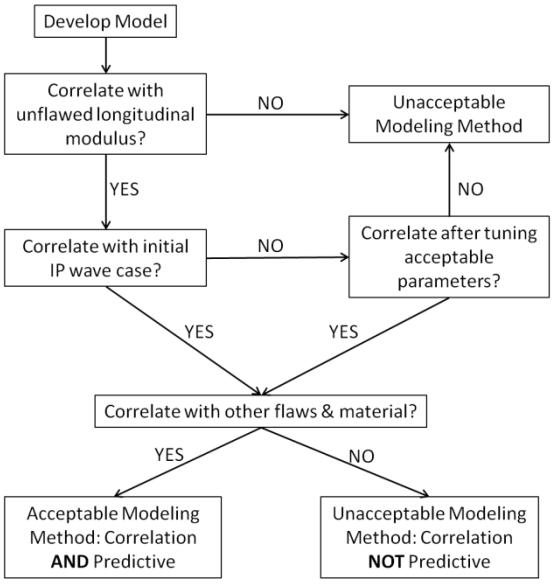

Figure 9. Flow chart depicting systematic approach to determine correlation acceptance (within 10% strain at peak stress) and predictive capability.

3.2 Modeling Methods

Several different modeling approaches were utilized and each is outlined below. For each approach, a baseline linear elastic model was used and the geometry was set up to match the intended coupon size (100 mm x 50 mm) established during the BMT. To determine if initial correlations were reasonable, 2D models (Figure) were generated with both unflawed and IP wave geometries, with quadrilateral, plane stress shell elements (S4R), in Abaqus where each element was generated to be consistent with the nominal fiber tow width (1.0 mm) [10]. The IP wave modeled had an amplitude (A) of 3.8 mm, a wavelength (λ) of 47.6 mm, and average off-axis fiber angle of 28.7°. Local coordinate systems were defined for the elements oriented to form the wave such that the fiber direction remained consistent through the wave, and the material properties were modeled to correctly match these properties. Displacement and boundary conditions were applied at the top and bottom, respectively, to match the BMT conditions and as such, full field calculations were set to match the BMT data for load-displacement and stress-strain correlations. Elastic material properties that were generated from the BMT discussed above were utilized as shown in Table 1. The geometry shown in Figure was utilized for all initial IP wave modeling efforts herein.

Table 1. Material properties generated during BMT.

	E_1	E_2	ν_1	G_{12}	G_{13}	G_{23}
Tension (GPa)	40.6	16.3	0.27	16.8	16.8	16.8
Compression (GPa)	38.4	14.4	0.28	14.4	14.4	14.4

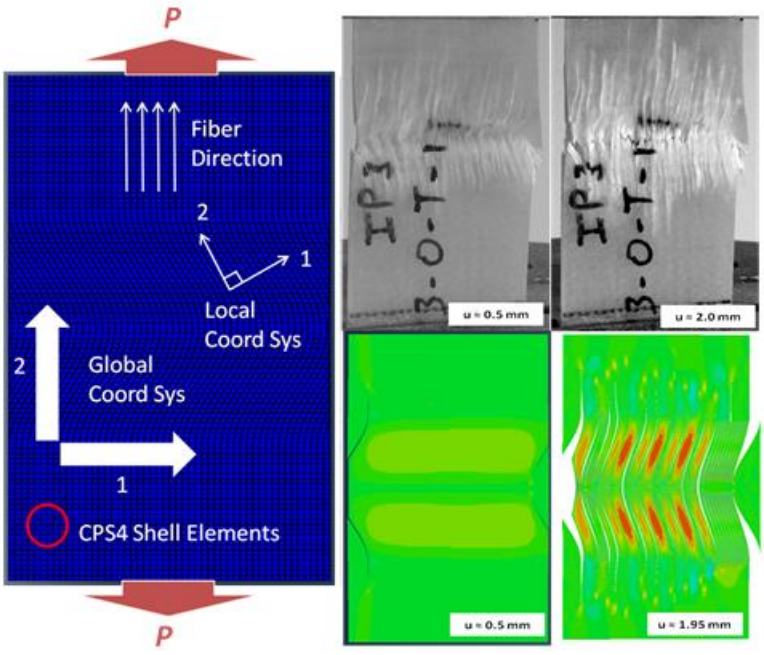

Figure 10. The 2D model setup utilized in the initial IP wave linear elastic models for each model (left) and comparison of damage between analytical (right-top) and experimental (right-bottom) showing onset and final damage left-to-right, respectively.

3.3 Results & Discussion

Several assumptions were made to simplify this modeling effort. First, it was assumed that all fibers were parallel and uniform in the intended direction with reference to the widthwise edge, including through the IP wave. It was also assumed that all the fibers, for both the unflawed and IP wave geometries, were parallel and aligned through the thickness. These assumptions greatly simplified the modeling approach even though they were a possible source of the variation noted within the BMT. In addition, perfect bonding between the layers was assumed. In the case of the IP wave, it was assumed that the initial failures and debonds of the discontinuous edge fibers had negligible effect on the material response and were disregarded for this effort.

As noted in the systematic approach, both qualitative and quantitative analysis was performed for each modeling technique. Qualitative correlation was assessed by utilizing visualized results from images and was noted immediately through the damage progression; an example is seen in Figure 10, right. In both the experimental and analytical cases, failure first occurs at the edges where fibers are discontinuous at low loads (Figure 10, right-top). Next, damage begins to accumulate in the area of fiber misalignment as the matrix, or cohesive elements, in that area begin to fail in shear as the fibers try to straighten due to the tensile load. The images below show analytical results at the same displacements points as the experimental images above (Figure 10, right-bottom). Due to the uniformity of model, the areas of failure are much cleaner and less complex. It is important to note that all modeling techniques had reasonable visual correlation that showed an initial progression of shear damage through the wavy section.

In order to perform quantitative analysis, stress-strain relationships as seen in **Error! Reference source not found.** were generated from each model utilizing a similar far-field strain as utilized for testing. Review of **Error! Reference source not found.** clearly indicates the differences in predicted response from the different modeling techniques. Table 2 offers identification of models run, acceptability of results, and both input parameters and acceptable parameters for tuning for each model. A summary of the results from each technique and an identification of the most accurate and consistent model are found below indicating that while some cases matched well, others did not. In particular, good correlation was noted for the Hashin failure criteria and combined modeling approaches, while the user-

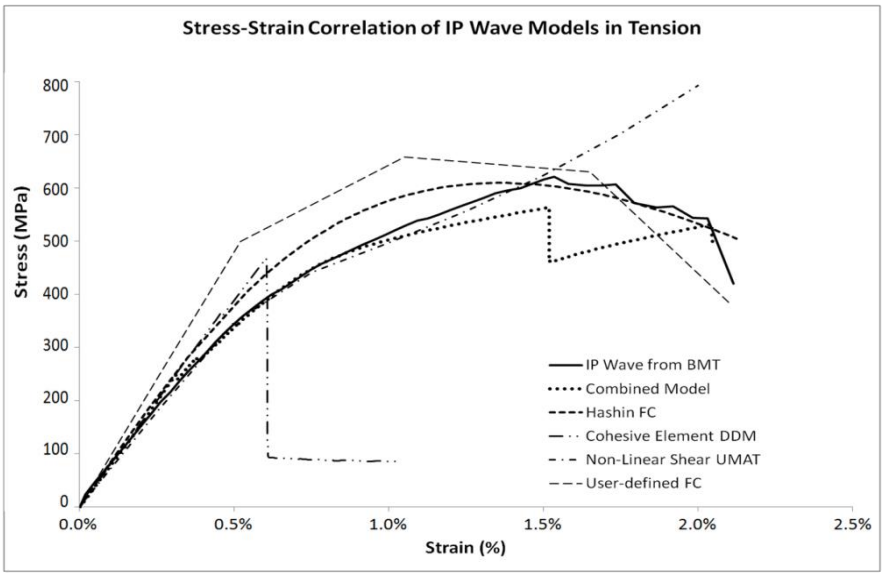

Figure 9. Stress-strain correlations of common IP Wave for each model technique compared to BMT results

defined failure criteria model, as implemented, showed poor correlation. More comprehensive details of, and results from, these models may be found in Reference [11].

To adequately compare the modeling techniques, Table 2 was created to show the results following the systematic approach employed and the results of each are discussed below. As noted in Table 2, a modulus check (MC) was performed in each case. Next, porosity was modeled using a true CDM approach where material properties were degraded based on amount of included air. Acceptable correlation (A) was achieved in tension, and while results appeared reasonable in compression, correlation was not performed (R) due to lack of consistency of BMT results. Given the property degradation model used, the lack of physical flaw geometry, and the acceptable correlation in tension, no additional runs or correlations were performed for porosity. As noted in Table 2, each technique was initially modeled with the same IP wave case, and if correlation was achieved, additional waves and materials were considered. Correlations were then performed except in cases where BMT results were insufficient, in which case the model was run (R) and correlation was left as future work when results are available. If correlation was deemed unacceptable (U), no additional cases were run.

Table 2. Identification of models run, acceptability of results, input parameters, and acceptable parameters for tuning.

			UNFLAWED		POROSITY		IP WAVE		OP WAVE		ADDITIONAL WAVES AND MATERIAL		INPUT PARAMETERS	TUNED PARAMETERS (ACCETABLE)
Model Type	Model	Effects of Defects Round	Tension	Comp	Tension	Comp	Tension	Comp	Tension	Comp	Tension	Comp		
CDM	Linear Elastic	1	MC	MC	NR	NR	NR	NR	NR	NR	NR	NR	ELASTIC PROPERTIES	NONE
	Linear Elastic w/ Hashin Failure Criteria	1	MC	MC	A	M	A	M	A	R	A,M	R	ELASTIC PROPERTIES & DAMAGE INITIATION, EVOLUTION, &	DAMAGE INITIATION, EVOLUTION, & STABILIZATION
	Subroutine w/ User defined Damage Criteria	2	MC	MC	NR	NR	U	U	NR	NR	NR	NR	ELASTIC PROPERTIES, REDUCED PROPERTIES, & FAILURE CRITERIA	REDUCED PROPERTIES
	Non-Linear Shear	2	MC	MC	NR	NR	U	U	NR	NR	NR	NR	ELASTIC PROPERITES & STRESS-STRAIN FROM UNFLAWED SHEAR RESPONSE	SUBTLE CHANGES TO STRESS-STRAIN
DDM	Cohesive Elements between Tows	2	MC	MC	NR	NR	U	U	NR	NR	NR	NR	ELASTIC PROPERTIES & COHESIVE TRACTION-SEPARATION	COHESIVE TRACTION-SEPARATION
Combined	Non-Linear Shear w/ Cohesive Elements between Tows	3	MC	MC	NR	NR	A	A	A	R	A	A,R	ELASTIC PROPERTIES, STRESS-STRAIN FROM UNFLAWED SHEAR RESPONSE, & COHESIVE TRACTION-SEPARATION	SUBTLE CHANGES TO STRESS-STRAIN & COHESIVE TRACTION-SEPARATION

KEY:
A = ACCEPTABLE CORRELATION (visual correlation and within 10% of Strain at Peak Stress while also within 10% of Peak Stress)
M = MODERATE CORRELATION (visual correlation but marginal quantitative acceptance criteria)
U = UNACCEPTABLE CORRELATION (unacceptable visual and/or quantitative correlation)
R = MODEL RUN BUT NOT CORRELATED (insufficient test data available)
NR = MODEL NOT RUN (due to unacceptable initial case or acceptable overall method)
MC = INITIAL MODULUS CHECK (stiffness of model within 5% of test)

Stepping through the modeling effort and results in Figure 11 and Table 2, first, a continuum based, linear elastic model was created and utilized to ensure that a standard model could match the modulus of elasticity of control samples from the BMT. This was considered to be a

continuum based approach because the individual materials (fiber and matrix) are not modeled separately but are instead modeled with smeared properties. Two model types with different laminates were run and correlated in tension and compression: a $[(0)_4]$ laminate and a $[0/\pm45/0]$ laminate. In both cases, correlation was achieved, confirming the model's ability to predict initial material stiffness response without the need for tuning of any parameters, verifying the model, and allowing for addition of damage progression.

The continuum based, linear elastic model initially utilized was modified to include damage progression built into Abaqus for the elastic-brittle nature of fiber-reinforced composites utilizing the Hashin criteria as noted above. Initially, two different models were created and utilized to model both the effects of porosity and an IP wave. In both cases, analytical/experimental correlation was noted, and in the case of porosity the correlation was sufficient and showed prediction potential warranting no further work. In the case of the IP wave, correlation was acceptable in certain regions depending on the amount and type of acceptable tuning of model variables and thus indicating that additional work with this technique was worthwhile (**Error! Reference source not found.**). Following the systematic approach, additional wave cases and a case with different material, a carbon fiber uni-directional, were generated and compared with BMT results as shown by the additional correlations in Table 2. In all cases, the model was able to consistently correlate to the initial IP wave case, not only indicating the promise of this technique but also verifying the systematic approach of increasing flaw complexity taken herein.

In an attempt to offer more user control compared to the built-in Hashin failure criteria, a similar model was created, swapping in a subroutine with user-defined failure criteria. Analytical/experimental correlations were made for the initial IP wave case and a significant amount of tuning, largely of the material property degradation scheme, was performed to attempt convergence. Given the amount of tuning necessary, this approach still resulted in poor correlation, as seen in **Error! Reference source not found.**. This modeling approach was found insufficient for predicting material response of an IP wave in tension or compression, and additional correlations were not deemed worthwhile as indicated in Table 2.

In addition, a CDM using a non-linear shear response and a DDM using cohesive elements, respectively, were each attempted. In both cases, analytical/experimental correlation was noted in specific areas of the stress-strain response (**Error! Reference source not found.**). The non-linear shear response model was able to capture the initial softening until fiber straightening resulted in divergence as longitudinal modulus became dominant. Similarly, the use of cohesive elements discretely realized matrix damage between the fiber tows, but implementation resulted in under-prediction of both peak stress and strain. In both cases, the models seemed to capture the initial response, while both lacked the exact damage progression observed in the BMT, and no additional correlations were attempted (Table 2).

Next, a model was created that combined the non-linear shear UMAT with cohesive elements placed between the fiber tows throughout the model. Analytical/experimental correlations were made and correlations were noted with the initial IP wave in both tension and compression. Following the systematic approach (Table 2), an OP wave and additional IP waves, including a carbon fiber case, were modeled and correlated showing the best combination of consistency, accuracy, and predictive capability. Correlation was achieved in each case without additional

tuning, as shown in Table 2 and **Error! Reference source not found.** indicating the promise of this modeling technique.

While it was quite clear that each model had some strengths, only the Hashin failure criteria and combined models proved to be acceptable and warranted following the systematic approach beyond the initial IP wave case. Looking at Table 2, it is evident that the Hashin failure criteria and combined model cases were the only two that correlated to the initial IP wave. The Hashin failure criteria results correlated well in tension after some tuning of the damage parameters; however, compression correlation was moderate. On the other hand, the combined model correlated well in both cases. Direct comparison of the results in tension (Figure 11) indicated that the combined model more accurately predicted damage and stress-strain response.

3.4 Crack Growth using the Multipoint Constraint Cohesive Model (MCM)

Material fracture can be modeled in the finite element method using special zero-thickness cohesive interface elements (CIEs) that represent crack openings by localizing displacement jumps at inter-element boundaries. Typically, cohesive elements are placed within the mesh along a well-defined and expected fracture path based on *a priori* knowledge of the problem, as for delamination of composite materials [12]. A more general approach is to insert CIEs between *all* conventional elements [13,14]. In this manner, the mesh intrinsically supports crack initiation and growth at all inter-element boundaries. Multiple cracks, fragmentation, and inhomogeneous materials are naturally permitted. However, the insertion of CIEs results in a substantial increase in the number of degrees of freedom (DOF) as well as the well-known problem of artificial compliance, even before the onset of damage. One means of counteracting the effect of artificial compliance is to choose very large values for the CIE initial "penalty" stiffness, K, such that the CIE becomes nearly rigid. Unfortunately, this leads to ill-conditioning of the global stiffness matrix. To avoid these issues, CIEs may be adaptively inserted while the solution progresses [15]; in this way fracture is extrinsically permitted. Unfortunately, remeshing and CIE insertion comes at a high computational cost. To address these issues, a novel approach combining advantages of both intrinsic and extrinsic cohesive models has been developed. Rather than using large penalty values of K a nodal master-slave constraint is imposed across the inter-element interface. This ensures exact displacement continuity across the interface prior to the onset of damage, and the solution is unaffected by the presence of "dormant" CIE. In addition, slave DOF are eliminated and the system is condensed to its original size. The MPCs may then be selectively deactivated using, for example, the stress output from immediately adjacent elements as a release criterion. Subsequent inter-element separation and damage evolution is then governed by an appropriate Traction-Separation relation.

In the following example, a typical 5-element membrane patch test [16] as shown in Figure 12a is used to illustrate differences between a conventional mesh, the proposed MCM, and the intrinsic cohesive mesh. Linear plane-strain elements are used with Young's Modulus, E=1.0 MPa, and Poisson's Ratio, ν=0.25. All exterior nodes are subjected to a prescribed displacement field of U_x=0.001(x+0.5y), U_y=0.001(0.5x+y). In this case, the patch test is passed if the displacements of the interior nodes (nodes 1-4) match the prescribed displacement field. The intrinsic and MCM models are derived from the conventional mesh by inserting zero-thickness CIEs, as indicated in Figure 12b and 12c, respectively. The results as K varies for the intrinsic model are displayed in the left column of Table 3. The displacement field plots are shown in

Figure 13 (for clarity, CIEs are not visualized). The absolute displacements, normalized (to the analytical solution) displacements, and the percent error are shown in Table 3. Clearly, the conventional and MCM models pass the displacement patch test. On the other hand, the intrinsic cohesive model exhibits severe displacement discontinuities even for very large *K*.

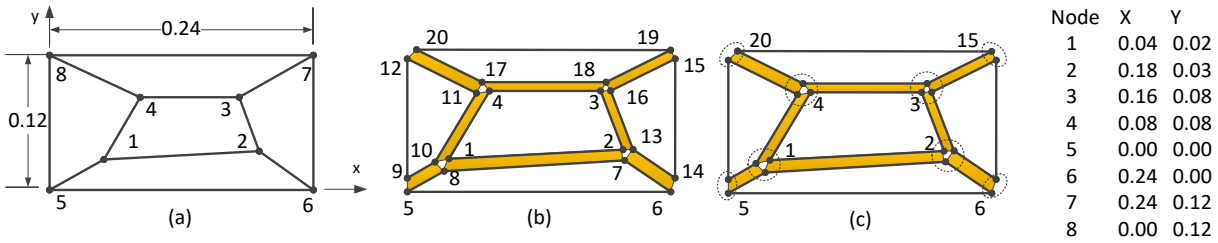

Figure 12. Example meshes showing nodes with "active" DOF; (a) Conventional, (b) Intrinsic, (c) MCM.

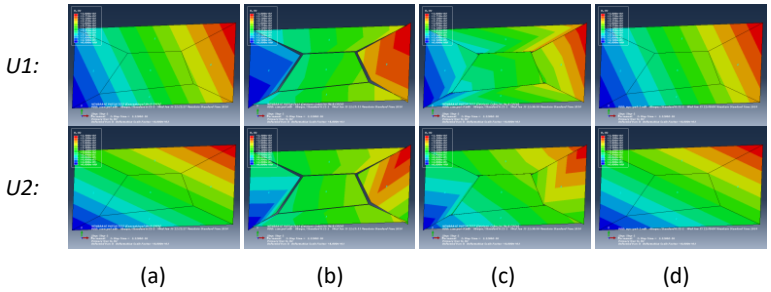

Figure 13. Patch test displacement plots; (a) Conventional, (b) Intrinsic (K=10·E), (c) Intrinsic (K=10^4·E), and (d) MCM. Scale factor=80.

Table 3. Summary of patch test displacement results.

Model	Node	U1	U2	Norm U1	Norm U2	%ERR U1	%ERR U2
Conventional	1	5.00E-05	4.00E-05	1.000	1.000	0.0	0.0
	2	1.95E-04	1.20E-04	1.000	1.000	0.0	0.0
	3	2.00E-04	1.60E-04	1.000	1.000	0.0	0.0
	4	1.20E-04	1.20E-04	1.000	1.000	0.0	0.0
Intrinsic K=10^1·E	1	1.08E-04	8.87E-05	2.156	2.217	115.6	121.7
	2	1.90E-04	1.60E-04	0.973	1.330	-2.7	33.0
	3	1.58E-04	1.47E-04	0.788	0.916	-21.2	-8.4
	4	1.20E-04	1.02E-04	0.999	0.848	-0.1	-15.2
Intrinsic K=10^4·E	1	7.70E-05	6.02E-05	1.540	1.505	54.0	50.5
	2	1.79E-04	1.30E-04	0.917	1.087	-8.3	8.7
	3	1.68E-04	1.54E-04	0.841	0.960	-15.9	-4.0
	4	1.46E-04	1.16E-04	1.214	0.966	21.4	-3.4
MCM K=10^1·E	1	5.00E-05	4.00E-05	1.000	1.000	0.0	0.0
	2	1.95E-04	1.20E-04	1.000	1.000	0.0	0.0
	3	2.00E-04	1.60E-04	1.000	1.000	0.0	0.0
	4	1.20E-04	1.20E-04	1.000	1.000	0.0	0.0

4. SUMMARY CONCLUSIONS & FUTURE WORK

While the probabilistic analysis has proved useful in addressing the uncertainty of manufacturing defects it must be performed with detailed and accurate information. For instance, this analysis

has shown the significance of flaw magnitude distributions. The analysis presented postulates that one should assess defects as a design parameter in a parametric probabilistic analysis. Results from this effort have shown that the probability of failure of a wind turbine blade with defects can be adequately described through the use of probabilistic modeling. The two approaches detailed in this analysis have shown that by treating defects as random variables one can reduce the design conservatism of a wind blade in fatigue. Reduction in the safe operating lifetime of a blade with defects, compared to one without, has shown that the inclusion of defects is critical for proper reliability assessment. If one assumes that defects account for some of the uncertainty in the blade design and these defects are analyzed with application specific data, then safety factors can be reduced.

This analysis has shown that the probability of failure is sensitive to the flaw magnitude distributions. Therefore, care must be taken to collect data specific to the structure and material system under scrutiny. The probabilistic analysis should be incorporated into a full reliability program that starts with an effort to investigate the Effects of Defects, then employ these results in a stochastic simulation process which aides the design process by establishing P_f, and finally utilize these results as a mechanism to evaluate defects during manufacturing and service life. Moreover, if embraced during the design and certification processes, probabilistic analysis can quantify uncertainty thereby reducing the reliance on arbitrary safety factors.

In addition, a unique comparison of several different analytical approaches to composites has been made with respect to manufacturing defects for consistency, accuracy, and predictive capability that will allow for improved blade reliability and composite structural assessment. A three-round, systematic approach of increasing complexity was utilized throughout. A benchmark material testing (BMT) program was performed to determine and characterize the material response when typical manufacturing flaws were included in representative wind turbine blade materials. Data from this program were then utilized as inputs and as correlation points for both continuum damage models (CDM) and discrete damage models (DDM). Following the three rounds of the BMT, models increased in complexity before a comparison of all correlations was performed.

Several conclusions may be drawn from the analytical work herein. Regardless of model type, initial laminate stiffness is easily calculated analytically when included flaw geometries are modeled discretely with the input of accurate unflawed material properties without any material response or failure criteria definitions. The simple CDM approach with Hashin failure criteria shows reasonably consistent, accurate, and predictive analytical/experimental correlation for a variety of fiber wave configurations with input of unflawed material properties and tuned damage properties from an initial case. The more complex CDM approaches with user-defined failure criteria resulted in inaccurate analytical/experimental correlation within the limits of acceptable parametric tuning. In addition, in the more complex CDM approach with non-linear shear UMAT and the DDM approach with cohesive elements placed between fiber tows, analytical approximations are able to capture initial softening, but they diverged from experimental results due to unrealistic responses. As such a combined approach was attempted with the non-linear shear UMAT CDM and the DDM approach with cohesive elements placed between fiber tows resulted in the most consistent, accurate, and predictive correlation. Further work is needed focusing on improving methodology and increasing scale. In particular, increased scale of models and testing will allow for correlation of models and testing to provide a

better understanding of flaw impacts on large structures which will be aided with such tools as the Cohesive Interface Element approach outlined herein.

5. REFERENCES

1. Cairns, D. S. Personal correspondence with wind turbine OEMs & blade manufactures
2. Hill, R. R., Peters, V. A., Stinebaugh, V. A., and Veers, P. S. "Wind Turbine Reliability Database Update" Sandia National Laboratory SAND2009-1171, 2009
3. Riddle, T.W., Nelson, J.W., & Cairns D.S. "Effects of Defects in Composite Wind Turbine Blades - Sandia Blade Reliability Collaborative", Sandia Report SAND2011-XXXX, 2011
4. Riddle, T. W. "DEVELOPMENT OF RELIABILITY PROGRAM FOR RISK ASSESSMENT OF COMPOSITE STRUCTURES TREATING DEFECTS AS UNCERTAINTY VARIABLES" PhD Thesis, Montana State University, Bozeman 2013.
5. *The SNL/MSU/DOE Fatigue of Composite Materials Database: Recent Trends.* Samborsky, D., Mandell, J., Miller, D.,. Honolulu : 53nd AIAA/ASME/ASCE/AHS/ASC Structures, Structural Dynamics and Materials Conference, 2012.
6. Nijssen. Fatigue life prediction and strength degredation of wind turbine rotor blade composistes. s.l. : Sandia National Labratories, 2007. SAND2006-7810P.
7. Nelson, J.W., Riddle, T.W., Cairns D.S. & Workman, J.E. (2012). Composite Wind Turbine Blade Effects of Defects: Part B—Progressive Damage Modeling of Fiberglass/Epoxy Laminates with Manufacturing Induced Flaws. 53nd AIAA/ASME/ASCE/AHS/ASC Structures, Structural Dynamics and Materials Conference; April 2012, Honolulu, HI.
8. Woo, K, Nelson, J.W., Cairns D.S. and Riddle, T.W., "Effects of Defects: Part B—Progressive Damage Modeling of Fiberglass/Epoxy Composite Structures with Manufacturing Induced Flaws Utilizing Cohesive Zone Elements." 54nd AIAA/ASME/ASCE/AHS/ASC Structures, Structural Dynamics and Materials Conference; April 2013, Boston, MA.
9. Lemanski, SL; J Wang, MPF Sutcliffe, KD Potter, & MR Wisnom (2012). Modelling failure of composite specimens with defects under compression loading. Composites Part A, v43, n3, pp. 435.
10. Abaqus Software/Documenation: v. 6.12; Dassault Systemes Simulia Corp, Providence, RI.
11. Nelson, J.W. "A COMPARISON OF CONTINUUM AND DISCRETE MODELING TECHNIQUES OF THE EFFECTS OF MANUFACTURING DEFECTS COMMON TO COMPOSITE STRUCTURES " PhD Thesis, Montana State University, Bozeman 2013.
12. Alfano, G.; Crisfield, M.A. (2001) Finite element interface models for the delamination analysis of laminated composites: mechanical and computational issues, International Journal for Numerical Methods in Engineering, 50; 1701-1736.
13. Ortiz, M.; Suresh, S. (1993) Statistical properties of residual stresses and intergranular fracture in ceramic materials, Journal of Applied Mechanics, 60; 77-84.
14. Xu, X.-P; Needleman, A. (1994) Numerical simulations of fast crack growth in brittle solids, Journal of the Mechanics and Physics of Solids, 42; 1397-1434.
15. Camacho, G. T.; Ortiz, M. (1996) Computational modelling of impact damage in brittle materials, International Journal of Solids and Structures, 33; 2899-2938.

16. Mandell, J.F.; Samborsky, D.D; Agastra, P.; Sears, A.T., and Wilson, T.J. (2010) Analysis of SNL/MSU/DOE fatigue database trends for wind turbine blade materials, SNL Report SAND2010-7052.